Kanglemycin A Can Overcome Rifamycin Resistance Caused by ADP-Ribosylation by Arr Protein

John Harbottle,[a] Hamed Mosaei,[a] Nicholas Allenby,[b] Nikolay Zenkin[a]

[a]Centre for Bacterial Cell Biology, Biosciences Institute, Faculty of Medical Sciences, Newcastle University, Newcastle upon Tyne, United Kingdom
[b]Odyssey Newcastle, The Biosphere, Draymans Way, Newcastle upon Tyne, United Kingdom

John Harbottle and Hamed Mosaei contributed equally to this work. Author order was determined alphabetically.

ABSTRACT Rifamycins, such as rifampicin (Rif), are potent inhibitors of bacterial RNA polymerase (RNAP) and are widely used antibiotics. Rifamycin resistance is usually associated with mutations in RNAP that preclude rifamycin binding. However, some bacteria have a type of ADP-ribosyl transferases, Arr, which ADP-ribosylate rifamycin molecules, thus inactivating their antimicrobial activity. Here, we directly show that ADP-ribosylation abolishes inhibition of transcription by rifampicin, the most widely used rifamycin antibiotic. We also show that a natural rifamycin, kanglemycin A (KglA), which has a unique sugar moiety at the *ansa* chain close to the Arr modification site, does not bind to Arr from *Mycobacterium smegmatis* and thus is not susceptible to inactivation. We, found, however, that kanglemycin A can still be ADP-ribosylated by the Arr of an emerging pathogen, *Mycobacterium abscessus*. Interestingly, the only part of Arr that exhibits no homology between the species is the part that sterically clashes with the sugar moiety of kanglemycin A in *M. smegmatis* Arr. This suggests that *M. abscessus* has encountered KglA or rifamycin with a similar sugar modification in the course of evolution. The results show that KglA could be an effective antimicrobial against some of the Arr-encoding bacteria.

KEYWORDS ADP-ribosylation, Arr, *Mycobacterium*, RNA polymerase, kanglemycin, rifampicin, rifamycin

Resistance to the front-line drug used in treatment of tuberculosis, rifampicin (Rif), is typically conferred through point mutations within the *rpoB* gene encoding the Rif-binding β-subunit of RNA polymerase (RNAP) (1). However, Rif is also subject to enzymatic inactivation by several recently described bacterial enzymes (2–5). ADP-ribosylation of Rif by *Mycobacterium smegmatis* rifampicin ADP-ribosyl transferase (Arr_{Ms}) is believed to preclude Rif binding to the RNAP β subunit, although this has not yet been directly demonstrated. Arr_{Ms} utilizes NAD^+ to catalyze the ADP-ribosylation of Rif at the C-23 hydroxyl group, with concurrent release of the nicotinamide moiety from NAD^+ (6) (Fig. 1A). Rifamycin SV, and the newer semisynthetic Rif derivatives rifaxamin and rifabutin, are also substrates for Arr_{Ms}, suggesting the enzyme has a broad substrate specificity for rifamycins (3, 7). However, it has been shown that C-25 carbamate derivatives of Rif exhibit greatly improved antimicrobial activity against *M. smegmatis* (8). *In vitro* experiments with purified Arr_{Ms} indicated that C-25 carbamate rifamycins are resistant to modification by Arr (8). The recently solved crystal structure of Arr_{Ms} in complex with Rif provides a rational explanation for this evasion of Arr inactivation; the supposed position of the C-25 carbamate group would afford a pronounced clash within the Arr_{Ms} Rif-binding pocket (3).

The emerging pathogen *Mycobacterium abscessus* is one of the most clinically important nontuberculous mycobacteria that are responsible for severe respiratory, skin, and
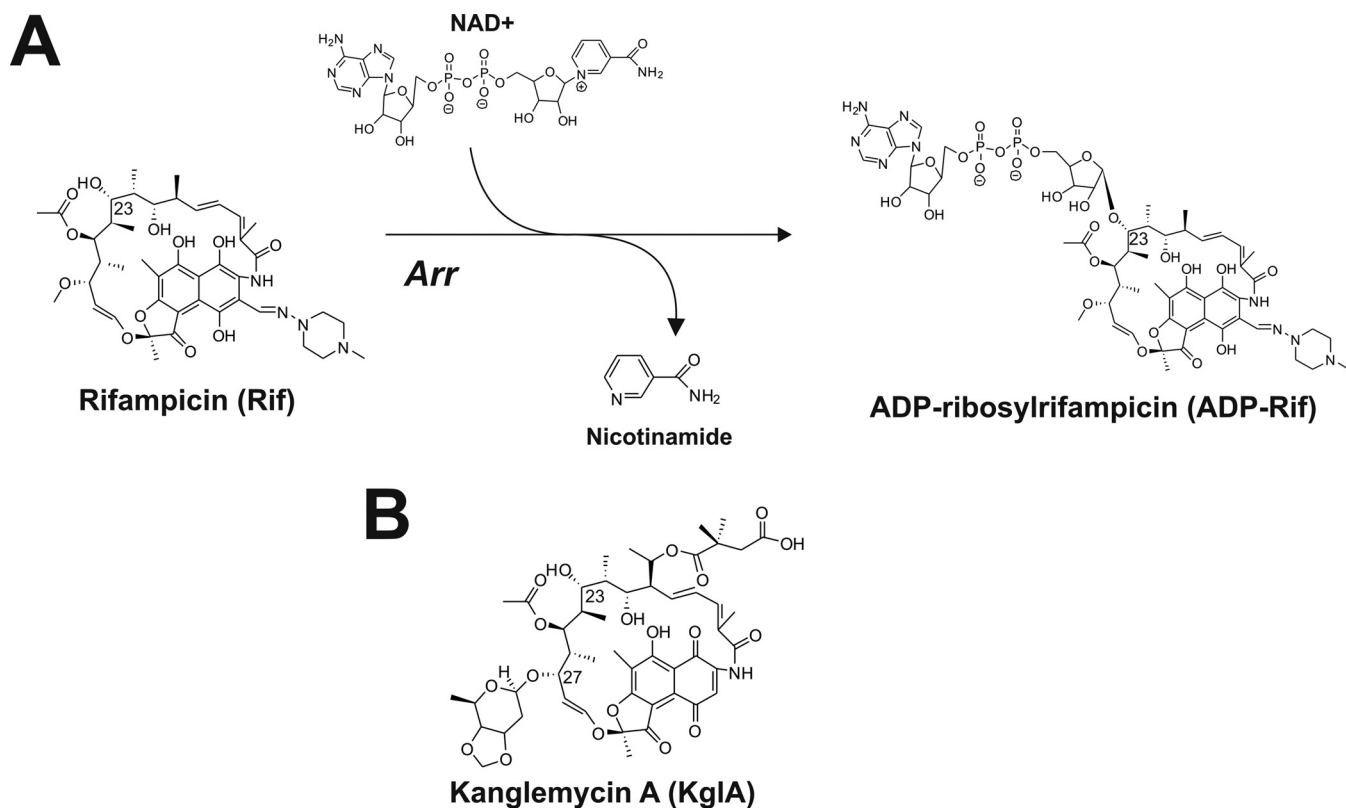
FIG 1 (A) ADP-ribosylation by rifampicin-ADP-ribosyl transferases (Arr) of rifampicin (Rif). (B) Structure of KglA.

mucosal infections in humans. Because of resistance to most classes of antibiotics, including rifamycins, infections caused by *M. abscessus* remain extremely difficult to treat (9). The genome of *M. abscessus* encodes a homologue of Arr_{Ms} (Arr_{Mab}) that confers innate high-level Rif resistance. Deletion of Arr_{Mab} significantly increases not only the sensitivity of *M. abscessus* to Rif but also that to other rifamycins, i.e., rifabutin, rifaximin, and rifapentine (7, 10, 11). Therefore, rifamycins that could evade the activity of Arr_{Mab} could be promising treatment candidates. The C-25-modified rifamycins have, similarly to Rif, high MICs against wild-type *M. abscessus* but considerably lower MICs against a mutant lacking Arr_{Mab} (11), suggesting that the putative Arr_{Mab} may have a different substrate specificity to Arr_{Ms}.

The natural product kanglemycin A (KglA) is an ansamycin antibiotic that, like other rifamycins, inhibits transcription by binding within the rifampicin-binding pocket on the β-subunit of RNAP (12). However, KglA has unique substituents present on the *ansa* bridge, namely, a 2,2-dimethylsuccinic acid chain at C-20 and a β-O-3,4-O,O' methylene digitoxose moiety at C-27. When bound to RNAP, these substituents afford additional binding contacts in the rifampicin-binding pocket and produce an altered binding conformation that leads to overcoming rifampicin-resistant amino acid substitutions (12).

We hypothesized that these large, bulky substituents may also prevent KglA binding to Arr or that the ADP-ribosylated KglA may be able to bind to RNAP due to its different mode of binding compared to that of Rif. In this study, we show that *M. smegmatis* Arr indeed cannot bind and modify KglA. In contrast, a homologue of Arr_{Ms} from *M. abscessus*, which we show is indeed a functional Rif ADP-ribosyl transferase, binds and modifies KglA with the same efficiency as that of Rif. We also, for the first time, directly show that ADP-ribosylated Rif does not inhibit bacterial RNAP.

RESULTS

***M. smegmatis* Arr (Arr_{Ms}) ADP-ribosylates Rif but not KglA.** In order to characterize Arr_{Ms} *in vitro*, we cloned the Arr gene from *M. smegmatis* into a pET28 expression

vector and expressed and purified the protein from *Escherichia coli*. To investigate the inactivation of antibiotics by Arr_{Ms}, we performed *in vitro* inactivation reactions with a tandem disk assay (Fig. 2A). Increasing concentrations of Arr_{Ms} were incubated with NAD^+ and antibiotic and then spotted onto paper disks which were placed onto a lawn of *Staphylococcus aureus* RN4220. Apparent decreases in the sizes of the zones of inhibition were interpreted as functional inactivation of the antibiotic. As shown in Fig. 2A, the control antibiotic carbenicillin is not inactivated by Arr_{Ms}. Rif is inactivated by Arr_{Ms}, resulting in decreased sizes of zones of inhibition when Arr_{Ms} concentration is increased. However, KglA appears to be resistant to inactivation by Arr_{Ms}, as the size of the zone of inhibition does not decrease even at very high concentrations of Arr_{Ms}. The results of the disc assay were corroborated by measurement of MIC for the drugs treated with Arr_{Ms} or left untreated (Table 1). Note that the smaller zones of inhibition and higher MICs seen with KglA, compared to those with Rif, is thought to be due to poorer penetration of the compound through the cell envelope. These data indicate that KglA is not a substrate for Arr_{Ms}.

To directly analyze ADP-ribosylation by Arr_{Ms}, we utilized a tandem liquid chromatography-mass spectrometry (LC-MS)-based assay in which antibiotic and NAD^+ substrates were incubated in the absence or presence of Arr_{Ms} and then the reaction products were separated by high-performance liquid chromatography (HPLC) and identified by mass spectrometry. When Rif is incubated with NAD^+ in the absence of Arr_{Ms}, Rif and its oxidized form rifampicin quinone (Rifq) are resolved with no identifiable ADP-ribosylated product (Fig. 2B). This indicates that the ADP ribosylation reaction requires enzymatic catalysis. Indeed, when incubated in the presence of NAD^+ and Arr_{Ms}, both Rif and Rifq are ADP-ribosylated, confirming the activity of purified Arr_{Ms} (Fig. 2B). Interestingly, however, incubation of KglA with NAD^+ and Arr_{Ms} failed to ADP-ribosylate KglA, indicating that KglA is not a substrate of Arr_{Ms} (Fig. 2C), which is consistent with results of the above-described *in vivo* assay.

M. abscessus Arr (Arr_{Mab}) ADP-ribosylates both Rif and KglA. Prior genetic experiments have indicated the substrate specificity of a putative ADP-ribosyl transferase from *M. abscessus*, Arr_{Mab}, may differ from that of Arr_{Ms} (11). Therefore, we aimed to determine the function and activity of Arr_{Mab} *in vitro*. First, a purified Arr_{Mab} was analyzed in the disk assay, as described above. As can be seen from Fig. 3A (middle row), Rif activity is almost completely eliminated by both concentrations of Arr_{Mab}, as judged by disappearance of the zone of inhibition when Rif is incubated with Arr_{Mab}. Unexpectedly, unlike Arr_{Ms}, Arr_{Mab} was also capable of inactivating KglA (Fig. 3A, bottom row). Measurement of MIC confirmed this observation (Table 1).

To resolve this apparent controversy, we directly analyzed activity of Arr_{Mab} using a tandem LC-MS-based assay, as we did for Arr_{Ms}. Incubation of Rif and Rifq with NAD^+ and Arr_{Mab} resulted in their ADP-ribosylation (Fig. 3B). However, unlike in the case with Arr_{Ms}, incubation of KglA with Arr_{Mab} and NAD^+ also resulted in ADP-ribosylation of the antibiotic (the exact mass of the product was 1,523.40 Da, the predicted mass of ADP-ribosyl KglA; Fig. 3C). This finding corroborates the results of the above-described disk assay. The results also confirm that the homologue of Arr_{Ms} from *M. abscessus* indeed encodes a functional rifamycin ADP-ribosyl transferase that has broader substrate specificity than that of Arr_{Ms}.

Rif and KglA binding affinities at Arr_{Mab} and Arr_{Ms}. The inability of Arr_{Ms} to ADP-ribosylate KglA can be explained by either inability to bind the KglA molecule or inability to perform the catalysis. To distinguish between these possibilities, we investigated the binding of Rif and KglA to Arr_{Ms} and Arr_{Mab} using microscale thermophoresis (MST). Apparent dissociation constants (K_d) were determined by titrating serial dilutions of antibiotics against Arr_{Ms} and Arr_{Mab}. The affinity of Arr_{Ms} to KglA was much lower than its affinity to Rif (Fig. 4A and B), suggesting that the bulky 2,2-dimethylsuccinic acid chain at C-20 and/or β-O-3,4-O,O′ methylene digitoxose at C-27 of KglA prevents binding of the compound to the Arr_{Ms} active site. In contrast, Arr_{Mab} bound both antibiotics with the same K_d. The result indicates that the inactivity of Arr_{Ms} toward KglA is explained by the reduced binding affinity to the antibiotic. Notably, Rif binds with greater affinity to
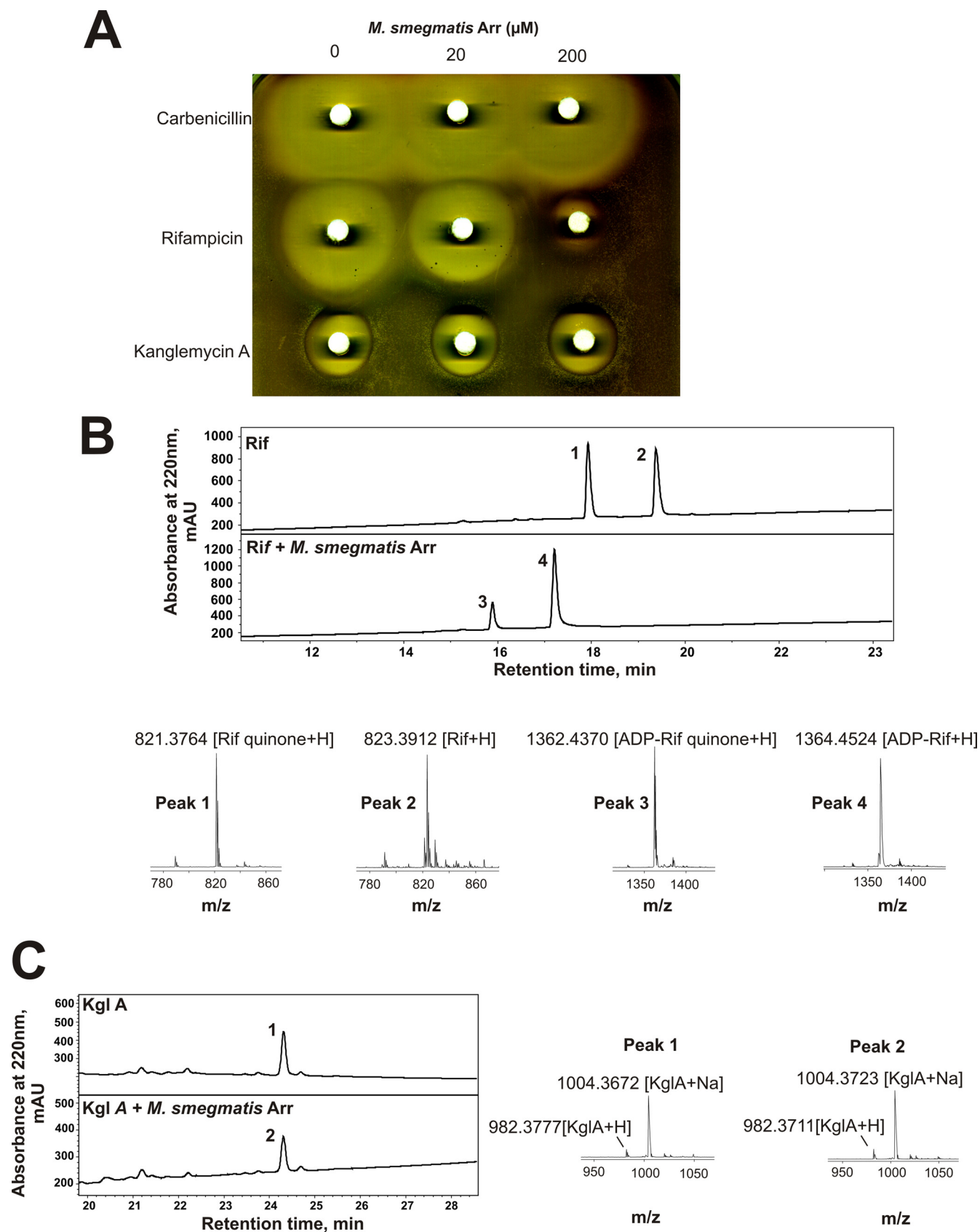
A

M. smegmatis Arr (µM)

0   20   200

Carbenicillin

Rifampicin

Kanglemycin A

B

Rif

Rif + M. smegmatis Arr

821.3764 [Rif quinone+H]

Peak 1

823.3912 [Rif+H]

Peak 2

1362.4370 [ADP-Rif quinone+H]

Peak 3

1364.4524 [ADP-Rif+H]

Peak 4

C

Kgl A

Kgl A + M. smegmatis Arr

Peak 1

1004.3672 [KglA+Na]

982.3777 [KglA+H]

Peak 2

1004.3723 [KglA+Na]

982.3711 [KglA+H]

FIG 2 *M. smegmatis* Arr (Arr$_{Ms}$) fails to inactivate kanglemycin A (KglA) by ADP-ribosylation. (A) Disk diffusion assay of aliquots of *in vitro* reaction mixtures with 1 mg/ml carbenicillin, rifampicin, or kanglemycin A incubated in the presence of indicated concentrations of Arr$_{Ms}$ in 10-μl reaction mixtures. Reaction

TABLE 1 MICs of Rif and KglA treated with Arr_{Sm} and Arr_{Mab} enzymes

Drug	MIC (μg/ml) of drug with:		
	No treatment	Treatment with *M. smegmatis* Arr	Treatment with *M. abscessus* Arr
Rif	0.007	>125	>125
KglA	0.488	0.488	>125

Arr_{Ms} than to Arr_{Mab} (Fig. 4A), suggesting that the broader substrate specificity of Arr_{Mab} comes at a cost of reduced binding affinity.

ADP-ribosylation renders rifamycins inactive against RNA polymerase. It is not known how ADP-ribosylation of rifamycins by Arr enzymes inactivates the antibiotics. Therefore, we purified ADP-ribosyl-Rif and ADP-ribosyl-KglA from the reactions catalyzed by Arr_{Ms} and Arr_{Mab}, respectively, and analyzed their effects on *in vitro* transcription by *E. coli* RNAP on a linear DNA template containing the T7A1 promoter. As can be seen in Fig. 5, consistently with our previous study (12), both Rif and KglA efficiently inhibited transcription with submicromolar 50% inhibitory concentrations (IC_{50}). In contrast, ADP-ribosyl-Rif and ADP-ribosyl-KglA were inactive even at high concentrations (100 μM). Because part of the mechanism of inhibition by all rifamycins is the sterical occlusion of the pathway of the nascent RNA (13), this result suggests that ADP-ribosylation prevents rifamycins binding to RNAP.

DISCUSSION

Rifamycins inhibit bacterial transcription by targeting the β-subunit of RNAP (13). One of the findings of this work is that ADP-ribosylation of Rif by Arr proteins completely abolishes its activity against RNAP *in vitro*. Addition of the ADP-ribosyl at C-23 abolishes a critical hydrogen bond between the Rif molecule and the RNAP and also orientates the bulky substituent toward the surface of the Rif-binding pocket on RNAP, likely causing a severe steric clash.

Importantly, however, we show that KglA, a rifamycin with unique bulky substituent present on the *ansa* bridge, is not a substrate for Arr_{Ms}, as a consequence of reduced binding affinity to the enzyme. If KglA adopts a similar conformation to that of Rif within the Rif-binding pocket of Arr_{Ms}, a strong steric clash occurs between the C-27 β-O-3,4-O,O' methylene digitoxose moiety of KglA and an α-helix (residues 54 to 65) that constitutes one half of the Rif-binding cleft of Arr_{Ms} (Fig. 6A). This α-helix, termed α1, is implicated in Rif-binding interactions; residue D55 makes polar interactions with O-11 of Rif, while residues A56, W59, G60, and L63 form nonpolar interactions with the carbon backbone of the *ansa* bridge (3). Arr homologues are widely distributed across various pathogenic and environmental bacteria (*E. coli*, *Pseudomonas aeruginosa*, *Klebsiella pneumoniae*, *Acinetobacter baumannii*, *Stenotrophomonas maltophilia*, *Burkholderia cenocepacia*, many anaerobic bacteria, and different actinomycetes species, such as *Streptomyces coelicolor*). Considering that KglA also retains activity against Rif-resistant RNAP and bacteria (12, 14), the antibiotic appears to be a promising lead compound with which to target some (but not all) bacteria possessing Arr enzymes.

We also characterized a homologue of Arr_{Ms} encoded by the *M. abscessus* genome and confirmed that it is a true ADP-ribosylase of Rif. Like Arr_{Ms}, Arr_{Mab} utilizes NAD^+ to catalyze the ADP-ribosylation of Rif. However, unlike Arr_{Ms}, KglA remains a substrate for

FIG 2 Legend (Continued)

mixtures were transferred onto the paper disks, which were placed on LB agar plates infused with a lawn of *S. aureus* RN4220 (8). (B) Reversed-phase high-performance liquid chromatography (HPLC) traces of *in vitro* modification of rifampicin (Rif) by Arr_{Ms}. Plots show Rif incubated with NAD^+ in the absence (upper trace) or presence (lower trace) of Arr_{Ms}. Below are the positive ion mass spectra of peaks 1, 2, 3, and 4. Ion adducts are as indicated. (C) Reversed-phase HPLC traces of KglA incubated with NAD^+ and with or without Arr_{Ms}, and mass spectra of peaks 1 and 2. Note that Rif and KglA have different absorbance spectra, and the areas or the heights of their chromatography peaks cannot be directly compared.
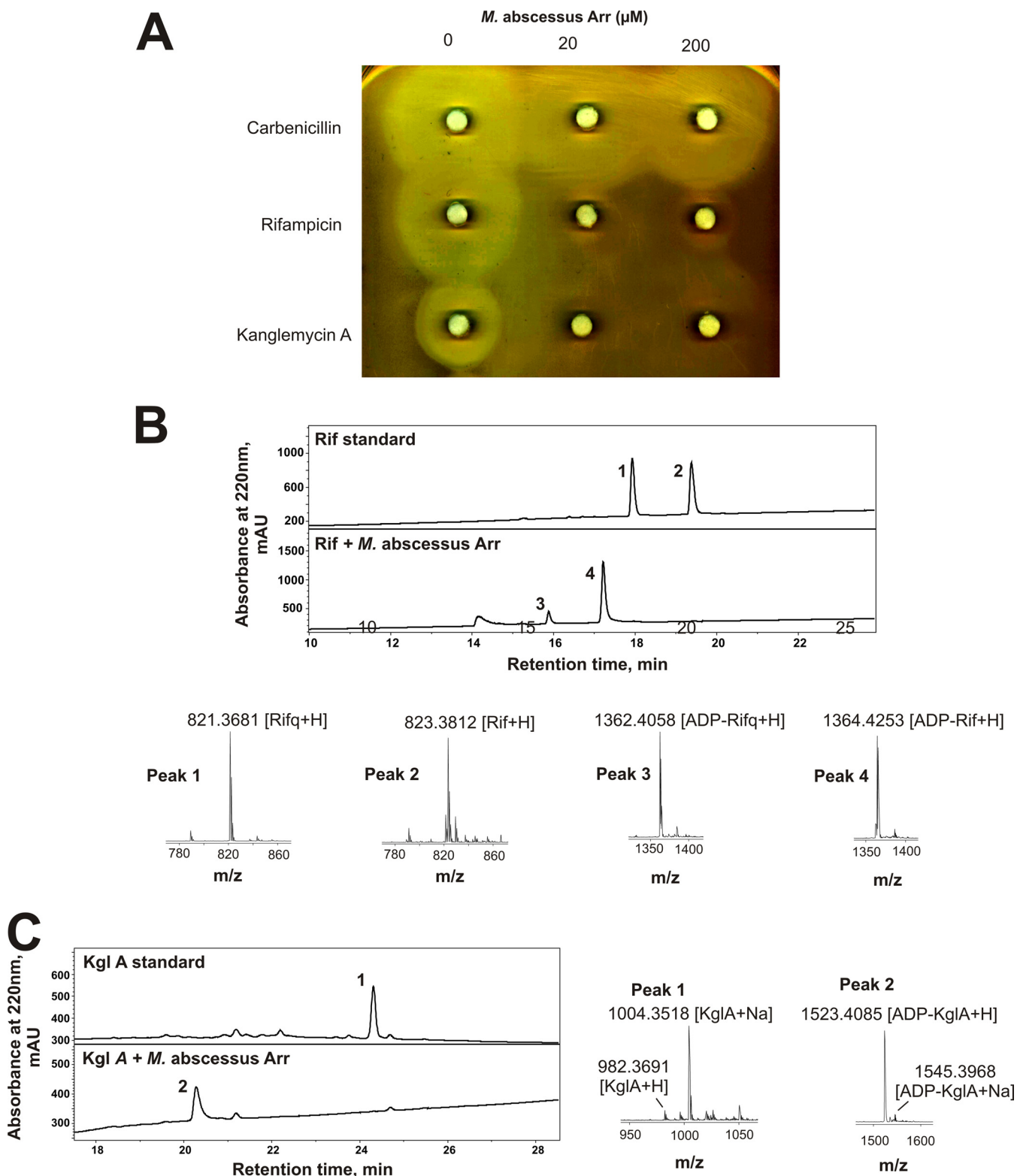
FIG 3 *M. abscessus* Arr (Arr$_{Mab}$) inactivates kanglemycin A (KglA) by ADP-ribosylation. (A) Disk diffusion assay of aliquots of *in vitro* reaction mixtures with 1 mg/ml carbenicillin, rifampicin, or kanglemycin A incubated in the presence of the indicated concentrations of Arr$_{Mab}$ in 10-μl reaction mixtures. Reaction mixtures were transferred onto the paper disks, which were placed on LB agar plates infused with a lawn of *S. aureus* RN4220. (B) Reversed-phase HPLC traces of *in vitro* modification of rifampicin (Rif) by Arr$_{Mab}$. Plots show Rif incubated with NAD$^+$ in the absence (upper trace) or presence (lower trace) of Arr$_{Mab}$. Below are the positive ion mass spectra of peaks 1, 2, 3, and 4. Ion adducts are as indicated. (C) Reversed-phase HPLC traces of KglA incubated with NAD$^+$ and with or without Arr$_{Mab}$, and mass spectra of peaks 1 and 2.
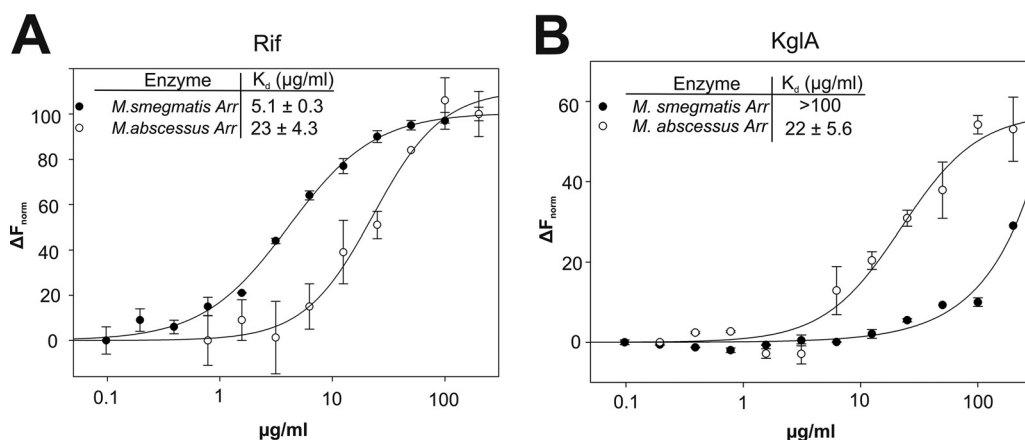
FIG 4 Substrate specificity of Arr$_{Ms}$ and Arr$_{Mab}$. Binding affinities of Rif (A) and KglA (B) at labeled Arr$_{Ms}$ and Arr$_{Mab}$, identified by microscale thermophoresis. Normalized fluorescence (F_{norm}; fluorescence after thermophoresis/initial fluorescence) is plotted against antibiotic concentration. Error bars $\pm$ standard deviation (SD) are shown.

ADP-ribosylation by Arr$_{Mab}$. The amino acid sequences between Arr$_{Ms}$ and Arr$_{Mab}$ are very similar, exhibiting a 66% sequence identity and 76% homology (Fig. 6B). However, Arr$_{Mab}$ α1 bears almost no sequence similarity with that of Arr$_{Ms}$. This lack of homology in α1 may underlie the broader substrate specificity exhibited by Arr$_{Mab}$. However, the variation of α1 residues involved in Rif binding may also explain the reduced affinity with which Arr$_{Mab}$ binds Rif (Fig. 4).

There is strong genomic evidence that most innate resistance mechanisms seen in clinical pathogens are of environmental origin (15). The often-communal existence of bacteria generates pressure to gain a competitive edge over neighboring microorganisms. Consequently, bacteria have evolved a number of mechanisms to counter antibiotics secreted by other microbes in their surroundings. Bulky ansamycin compounds, such as KglA, are produced by actinomycetes that occupy the same natural niches as nontuberculous mycobacteria, such as *M. abscessus* (14, 16). It is tempting to speculate that in its evolution, *M. abscessus* has encountered KglA or a similar natural rifamycin with a modified *ansa* bridge.
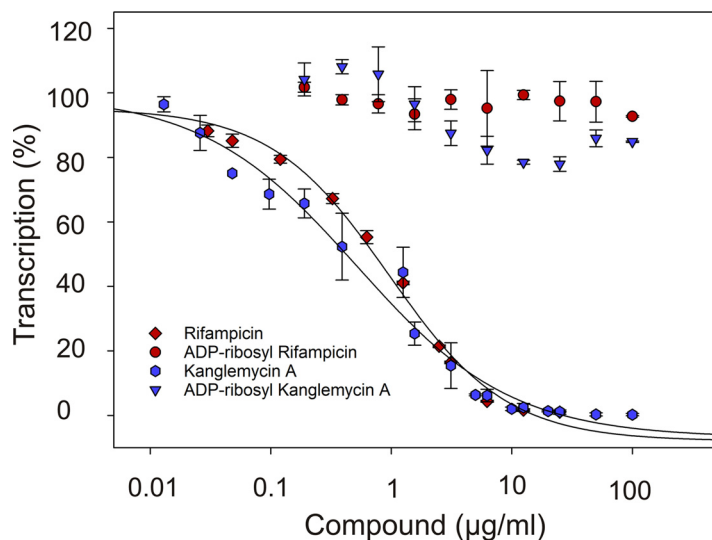

FIG 5 ADP-ribosylated rifamycins fail to inhibit RNAP. Effects of Rif and KglA and ADP-ribosylated Rif and KglA on *in vitro* transcription by *E. coli* RNAP on a linear DNA template containing the T7A1 promoter. Runoff and terminated transcription products were normalized to those synthesized in the absence of inhibitor. Error bars $\pm$ SD are shown.

A

B

```
                                                                                    α1
M. smegmatis PKPFEVHESGAYLHGTKAELKVGDRLVPGRESNFEAGRIMNHIYITQTLDAAVWGAELAA
             P  FE HESGAY HGTKA+L +GD L PG  SN+E GR+MNHIY+T+TL A   A +A
M. abscessus PNFFEAHESGAYFHGTKADLAIGDLLTPGHLSNYEEGRVMNHIYVTKTLVGAGLAAMMAK

M. smegmatis GEGRGRIFIVEPEGAIEDDPNVTDKKLPGNPTRSYRTREPVWIVGELTDWVGHPPEQLAA
             GEGRG ++IVEPEG +EDDPNVTDKK PGNPT SYR+REPV IVGE+ DW G PPE +
M. abscessus GEGRGHVYIVEPEGTLEDDPNVTDKKFPGNPTHSYRSREPVRIVGEVLDWEGPPPEFMET

M. smegmatis MRQGLEELRRKGLAVIYD  143
             R GL +L+RKG AVIYD
M. abscessus FRAGLADLKRKGNAVIYD  141
```
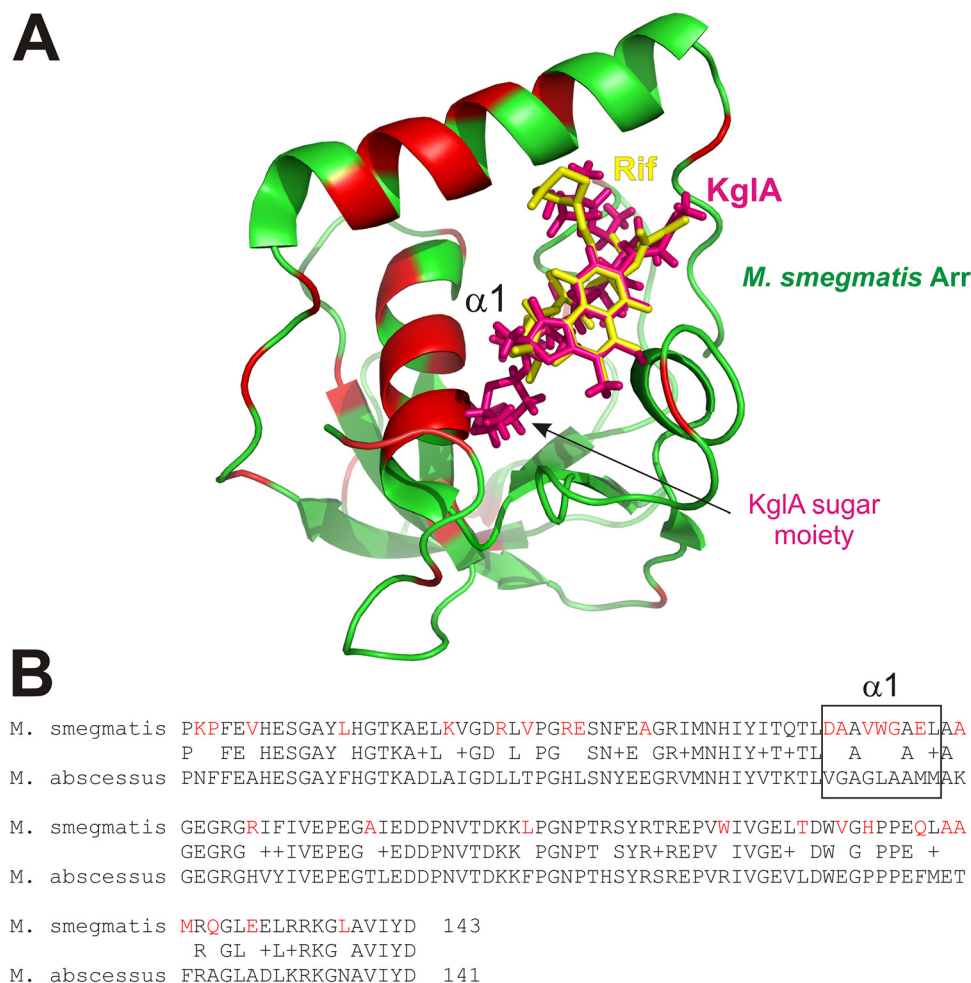
FIG 6 (A) Structural alignment of the KglA molecule (magenta) and Rif (yellow) complexed with *M. smegmatis* Arr (green; PDB identifier 2HW2) (3). Red patches show absence of homology with $Arr_{Mab.}$ (B) Sequence alignment of Arr_{Ms} and $Arr_{Mab.}$ Alpha helix 1 (α1) is highlighted.

It should be noted that the precise physiological role of Arr enzymes remains unclear, as Arr has been shown to play roles in cellular pathways even in the absence of rifamycins. For example, Arr is upregulated in response to different stresses (e.g., double-stranded DNA breaks, starvation, oxidative stress, and ciprofloxacin treatment) (17). In *M. smegmatis*, Arr contributes to biofilm formation and confers a growth fitness advantage. Although its expression has been shown to be associated with the stringent response, the mechanism of stress-correlated gene induction is unclear (18). It is possible that the main function of Arr is still inactivation of rifamycins, but the presence of rifamycins causes similar cell stresses (such as double-strand breaks caused by collisions of RNAP with replication machinery) that signal for production of Arr.

MATERIALS AND METHODS

Reagents, antibiotics, and DNA templates. All chemicals, reagents, and antibiotics were purchased from Sigma unless otherwise stated. The T7A1 promoter fragment was produced by PCR with the primers 5′-CGACGTTGTAAAACGACGGCCAGTG-3′ and 5′-GGTCGACTCTAGAGGATCGCT-3′ (IDT) from the template GGTCGACTCTAGAGGATCGCTATAACAGGCCTGCTGGTAATCGCAGGCCTTTTTATTTGGATCCAGATCCCGAAAA-TTTATCAAAAAGAGTATTGACTTAAAGTCTAACCTATAGGATACTTACAGCCATCGAGAGGGACACGGCGAATAGCC-ATCCCAATCGACACCGGGGTCCGGGATCTGGATCTGGATCGCTAATAACAGGCCTGCTGGTAATCGCAGGCCTTTTT-ATTTGGATCCCCGGGTACCGAGCTCGAATTCACTGGCCGTCGTTTTACAACGTCG and was purified by agarose gel electrophoresis. Kanglemycin A was purified as described previously (12).

Protein expression and purification. *E. coli* RNAP core and σ^{70} were purified exactly as described previously (19). *M. smegmatis* and *M. abscessus* Arr were expressed in T7 express cells (New England Biolabs) transformed with pET28 expression vector encoding N-terminal 6×His-tagged *M. smegmatis* Arr or *M. abscessus* Arr. Expression was induced with 0.4 mM isopropyl-β-D-thiogalactopyranoside (IPTG) in exponentially growing cells, which were then incubated overnight at room temperature on an orbital shaker (150 rpm). Cells were then harvested by centrifugation and resuspended in grinding buffer (50 mm Tris-HCl [pH 7.9], 10% glycerol, 200 mM NaCl, and protease inhibitor mixture [Roche]). Cells were then lysed by sonication and debris cleared by centrifugation. Arr enzymes were then purified by HisTrap HP (Cytiva) nickel affinity chromatography, concentrated, and dialyzed into storage buffer (50 mM Tris-HCl [pH 7.9], 50% glycerol, 200 mM NaCl, and 2 mM β-mercaptoethanol).

In vitro rifampicin ADP-ribosyl transferase activity assay. Reactions were performed in a 100-μl final volume of Arr buffer (20 mM Tris-HCl [pH 7.9], 40 mM KCl, and 0.5 mM MgCl$_2$). *M. smegmatis* or *M. abscessus* Arr (10 μM) was mixed with Rif or KglA (100 μM) in 80 μl of Arr buffer at 37°C for 10 min. A 20-μl aliquot of NAD$^+$ in Arr buffer was added (250 μM final) and incubated for 1 h at 37°C. The reaction was quenched with 500 μl of methanol (MeOH). Methanol was then evaporated under negative pressure and the reaction mixture analyzed by LC-MS. All analytical separations were performed on an Agilent 1260 HPLC instrument by injection of 1 to 5 μl of sample onto a Raptor ARC-18 column (150 mm by 2.1 mm) (Restek) or an Ultra C$_4$ column (150 mm by 2.1 mm) operated at 0.2 μl/min and then eluted using a 30-min linear gradient from 5% to 100% of acetonitrile. The mobile phase was supplemented with 0.1% formic acid. Mass spectra were recorded in positive-ion mode on a Bruker MicrOTOF II time-of-flight mass spectrometer.

Rifampicin ADP-ribosyl transferase disk assay. Reactions were performed in a 10-μl final volume of Arr buffer. *M. smegmatis* or *M. abscessus* Arr at an indicated concentration (0 μM, 20 μM, or 200 μM) was mixed with antibiotic (1 mg/ml final) in 8 μl Arr buffer at 37°C for 5 min. A 2-μl aliquot of NAD$^+$ in water was added (10 mM final) and incubated for 1 h at 37°C. The reaction was quenched with an equal volume of methanol, the mixture spotted onto paper disks, and a disk assay performed with an embedded lawn of *S. aureus* RN4220 as described previously (20).

Rifampicin ADP-ribosyl transferase MIC assay. MICs were quantified by broth microdilution assay using the *S. aureus* RN4220 strain at a starting cell density of 2×10^5 to 5×10^5 CFU/ml and tryptic soy broth (Oxoid). The compounds were dissolved in dimethyl sulfoxide (DMSO). Cultures were incubated for 24 h at 37°C, and MIC was recorded as the lowest concentration of each drug leading to inhibition of visible growth. Reproducibility was ensured by repeating all tests at least twice on separate occasions.

Purification of ADP-ribosyl rifampicin. The reaction was performed in a 2,000-μl volume of Arr buffer containing 25 μM *M. smegmatis* Arr, 5 mg rifampicin, and 20 mM NAD$^+$. The reaction mixture was incubated at 37°C for 24 h and cleaned up on a 25 ml HyperSep C$_8$ solid-phase extraction (SPE) cartridge. ADP-ribosylated Rif was eluted with 30% MeOH and dried under negative pressure to yield 4.8 mg of ADP-ribosyl-Rif. Sample homogeneity was confirmed by tandem LC-MS, as described above.

In vitro transcription. Transcription from promoter DNA fragments was performed essentially as described previously (12, 19). Reactions were performed in 10 μl of transcription buffer TB (20 mM Tris HCl [pH 7.9], 40 mM KCl, and 10 mM MgCl$_2$) containing 1 pmol of *coli* RNAP core with 3 pmols of σ^{70} and 10% DMSO with or without inhibitors. Transcription was initiated by the addition of a mixture of 25 μM CpA dinucleotide as a primer, 0.2 μl α-[^{32}P] UTP (10 mCi/ml; Hartmann Analytic), 10 μM UTP, 100 μM ATP, 100 μM CTP, and 100 μM GTP, and 10 nM promoter DNA. Reactions were stopped after 10-min incubation at 37°C by the addition of equal volume of formamide-containing loading buffer. Products were resolved in denaturing polyacrylamide gels, revealed by phosphorimaging (Cytiva), and analyzed using ImageQuant software (Cytiva).

Microscale thermophoresis. Binding affinity experiments were carried out on a Monolith NT.115 series instrument (Nano Temper Technologies GMBH). *M. smegmatis* and *M. abscessus* Arr were labeled with Monolith Protein labeling kit RED-NHS second-generation amine (Nano Temper Technologies GMBH) according to the manufacturer's guidelines. Roughly 5 μl of sample in MST buffer (20 mM HEPES [pH 7.9], 40 mM KCl, and 10 mM MgCl$_2$) were loaded into Monolith NT.115 Premium capillaries, and thermophoresis was measured for 30 s. Analysis was performed with Monolith software. K_d was quantified by analyzing the change in normalized fluorescence (F_{norm}; fluorescence after thermophoresis/initial fluorescence) as a function of inhibitor concentration. Curves for K_d data were fitted to a 4-parameter logistic equation using nonlinear regression in SigmaPlot software.

REFERENCES

1. Campbell EA, Korzheva N, Mustaev A, Murakami K, Nair S, Goldfarb A, Darst SA. 2001. Structural mechanism for rifampicin inhibition of bacterial RNA polymerase. Cell 104:901–912. https://doi.org/10.1016/s0092-8674(01)00286-0.

2. Spanogiannopoulos P, Thaker M, Koteva K, Waglechner N, Wright GD. 2012. Characterization of a rifampin-inactivating glycosyltransferase from a screen of environmental actinomycetes. Antimicrob Agents Chemother 56:5061–5069. https://doi.org/10.1128/AAC.01166-12.

3. Baysarowich J, Koteva K, Hughes DW, Ejim L, Griffiths E, Zhang K, Junop M, Wright GD. 2008. Rifamycin antibiotic resistance by ADP-ribosylation: structure and diversity of Arr. Proc Natl Acad Sci U S A U S A U S A 105: 4886–4891. https://doi.org/10.1073/pnas.0711939105.

4. Liu L-K, Abdelwahab H, Martin Del Campo JS, Mehra-Chaudhary R, Sobrado P, Tanner JJ. 2016. The structure of the antibiotic deactivating, N-hydroxylating rifampicin monooxygenase. J Biol Chem 291:21553–21562. https://doi.org/10.1074/jbc.M116.745315.

5. Stogios PJ, Cox G, Spanogiannopoulos P, Pillon MC, Waglechner N, Skarina T, Koteva K, Guarné A, Savchenko A, Wright GD. 2016. Rifampin phosphotransferase is an unusual antibiotic resistance kinase. Nat Commun 7:11343. https://doi.org/10.1038/ncomms11343.

6. Morisaki N, Hashimoto Y, Furihata K, Imai T, Watanabe K, Mikami Y, Yazawa K, Ando A, Nagata Y, Dabbs ER. 2000. Structures of ADP-ribosylated rifampicin and its metabolite: intermediates of rifampicin-ribosylation by Mycobacterium smegmatis DSM43756. J Antibiot 53:269–275. https://doi.org/10.7164/antibiotics.53.269.

7. Agrawal P, Miryala S, Varshney U. 2015. Use of Mycobacterium smegmatis deficient in ADP-ribosyltransferase as surrogate for Mycobacterium tuberculosis in drug testing and mutation analysis. PLoS One 10:e0122076. https://doi.org/10.1371/journal.pone.0122076.

8. Combrink KD, Denton DA, Harran S, Ma Z, Chapo K, Yan D, Bonventre E, Roche ED, Doyle TB, Robertson GT, Lynch AS. 2007. New C25 carbamate rifamycin derivatives are resistant to inactivation by ADP-ribosyl transferases. Bioorg Med Chem Lett 17:522–526. https://doi.org/10.1016/j.bmcl.2006.10.016.

9. Johansen MD, Herrmann JL, Kremer L. 2020. Non-tuberculous mycobacteria and the rise of Mycobacterium abscessus. Nat Rev Microbiol 18: 392–407. https://doi.org/10.1038/s41579-020-0331-1.

10. Schafle D, Selchow P, Borer B, Meuli M, Rominski A, Schulthess B, Sander P. 2021. Rifabutin is inactivated by Mycobacterium abscessus Arr. Antimicrob Agents Chemother 65:e02215-20. https://doi.org/10.1128/AAC.02215-20.

11. Rominski A, Roditscheff A, Selchow P, Bottger EC, Sander P. 2017. Intrinsic rifamycin resistance of Mycobacterium abscessus is mediated by ADP-ribosyltransferase MAB_0591. J Antimicrob Chemother 72:376–384. https://doi.org/10.1093/jac/dkw466.

12. Mosaei H, Molodtsov V, Kepplinger B, Harbottle J, Moon CW, Jeeves RE, Ceccaroni L, Shin Y, Morton-Laing S, Marrs ECL, Wills C, Clegg W, Yuzenkova Y, Perry JD, Bacon J, Errington J, Allenby NEE, Hall MJ, Murakami KS, Zenkin N. 2018. Mode of action of kanglemycin A, an ansamycin natural product that is active against rifampicin-resistant Mycobacterium tuberculosis. Mol Cell 72:263–274.e265. https://doi.org/10.1016/j.molcel.2018.08.028.

13. Mosaei H, Zenkin N. 2020. Inhibition of RNA polymerase by rifampicin and rifamycin-like molecules. EcoSal Plus 9. https://doi.org/10.1128/ecosalplus.ESP-0017-2019.

14. Peek J, Lilic M, Montiel D, Milshteyn A, Woodworth I, Biggins JB, Ternei MA, Calle PY, Danziger M, Warrier T, Saito K, Braffman N, Fay A, Glickman MS, Darst SA, Campbell EA, Brady SF. 2018. Rifamycin congeners kanglemycins are active against rifampicin-resistant bacteria via a distinct mechanism. Nat Commun 9:4147. https://doi.org/10.1038/s41467-018-06587-2.

15. Peterson E, Kaur P. 2018. Antibiotic resistance mechanisms in bacteria: relationships between resistance determinants of antibiotic producers, environmental bacteria, and clinical pathogens. Front Microbiol 9:2928. https://doi.org/10.3389/fmicb.2018.02928.

16. Honda JR, Virdi R, Chan ED. 2018. Global environmental nontuberculous mycobacteria and their contemporaneous man-made and natural niches. Front Microbiol 9:2029–2029. https://doi.org/10.3389/fmicb.2018.02029.

17. Stallings CL, Chu L, Li LX, Glickman MS. 2011. Catalytic and non-catalytic roles for the mono-ADP-ribosyltransferase Arr in the mycobacterial DNA damage response. PLoS One 6:e21807. https://doi.org/10.1371/journal.pone.0021807.

18. Agrawal P, Varada R, Sah S, Bhattacharyya S, Varshney U. 2018. Species-specific interactions of Arr with RplK mediate stringent response in bacteria. J Bacteriol 200:e00722-17. https://doi.org/10.1128/JB.00722-17.

19. Harbottle J, Zenkin N. 2020. Ureidothiophene inhibits interaction of bacterial RNA polymerase with −10 promotor element. Nucleic Acids Res 48: 7914–7923. https://doi.org/10.1093/nar/gkaa591.

20. Bauer AW, Kirby WM, Sherris JC, Turck M. 1966. Antibiotic susceptibility testing by a standardized single disk method. Am J Clin Pathol 45:493–496. https://doi.org/10.1093/ajcp/45.4_ts.493.